Jestr

Journal of Engineering Science and Technology Review 7 (2) (2014) 113 – 118

JOURNAL OF
Engineering Science and Technology Review

www.jestr.org

Research Article

Finite element simulation of shallow-buried and mining tunnelling in adjacent frame structures

Chun-lai Chen[1], Qi Ye[1], Nan-ting Yu[1], Gang Wei[1,*] and Hui-hui Hu[2]

[1] *Department of Civil Engineering, Zhejiang University City College, 310015, Hangzhou, China*
[2] *Department of Civil and Structural Engineering, The Hong Kong Polytechnic University, Hong Kong*

Received 15 February 2014; Accepted 23 May 2014

Abstract

By using three dimensional software MIDAS/GTS, the interactions among structures-soil-tunnel system is considered in this paper, and the working condition of shallow-buried underground excavation is simulated in the foundation of frame structures with the short-pile. The loadings and deformations of structures are studied before and after the tunnelling, and the influences of the following factors, including the horizontal position of tunnel and building, the height of building and the soil property, are analyzed. It is indicated that when the horizontal distance L equals zero (the distance between building axis to the tunnel axis), the building settlement increases gradually and shows a normal distribution during and after the tunnelling. Due to the small stiffness of frame structures with short-pile foundations, the building has large non-uniform settlement. When the distance of excavation is no less than 1.8 times of the thickness of overburden soil, the building settlement becomes stable, and the first principal stress P_1 and maximum deformation rate E_1 generally show a trend of decrease. With the increasing L, P_1 and E_1 will decrease accordingly, and the buildings tend to be inclined toward the tunnel. For a relatively larger distance, the building is nearly not affected.

Keywords: Shallow-buried underground excavation; Finite element method; Frame structure; Short-pile foundation

1. Introduction

Because of the heavy transportation in many major cities of China, the underground tunnels have attracted significant attentions and efforts. Shield method [1] and shallow-buried underground excavation method [2] are commonly used in underground tunnel construction. For the densely distributed structures and underground pipelines, the effects caused by the shallow-buried and mining tunneling are hardly avoidable, which may result in inclination, cracking or even collapsing of adjacent structures [3]. In order to ensure the safety of structures, it is important to monitor the variation of displacement and stress in the soil and structures during the tunneling. At present, the main research methods about the influences of underground tunnel construction on nearby buildings include the analytical method [2], [4], [5] and the finite element method [6], [7], [8], [9], [10], [11], [12], [13], [14], [15], etc. It is found that the present research mainly concentrates on the shield tunnel [6], [7], [8], [9], [10], [11], [12], [13], and there are few researches considering the shallow-buried underground tunnel. Besides, the previous researches mainly focus on shallow tunnel road surface settlements caused by shallow-buried underground tunnel construction, and no works have been carried out on the structure stress and deformation due to the construction of shallow-buried underground tunnel.

The three-dimensional MIDAS/GTS software is used in the present paper which simulates the working condition of shallow-buried excavation tunnel which vertically crosses through the foundation of the frame structures with short-piles. The loadings and deformations of buildings before and after the excavation of tunnel face is studied, and the influences resulted from the change of horizontal position of tunnels and buildings, the height of building and the soil property are analyzed.

2. Three Dimensional Finite Element Method

2.1 Models and the short-cut process of parameter

The thickness of covered soil of shallow-buried underground tunnel h is 12 m and the diameter is 6m. The excavation is performed by using the benching excavation method, and pre-reinforcement area ahead of excavation face is 2 m. The distance between up- and down-side excavation is 6 m. The thickness of pre-reinforcement zone is 1.5 m. The primary support thickness of tunnel is 0.3 m and shot concrete C25 is used. Considering that concrete shifted from soft to hard during construction process, the attribute of initial stage was set as primary support (soft) and the attribute after hardened was set as primary support (hard). The thickness of tunnel face and the temporary steel is 0.12 m.

The building is a reinforced concrete frame structure with 4 ground layers. The thickness of each layer is 3.6 m

* E-mail address: weig@zucc.edu.cn

ISSN: 1791-2377

(including the thickness of the floor). The C30 concrete was adopted. There are 5 bays each being of 6.6 m in the horizontal direction and 2 bays of 6.3 m in the longitudinal direction (direction along the tunnel drilling). The cross section of the columns is 0.4 m*0.4 m, and the beam is 0.3 m*0.55 m. The thickness of the floor is 0.1 m. The Short-pile foundation is adopted with caps. The cap is 1 m in height, 2 m in width and 2 m in length, while the short-pile has a length of 6 m and a diameter of 1.2 m. The C35 concrete is also adopted as shown in Figure 1. The effects of the inner wall on the lateral stiffness of frame structure are not considered [16]. Instead, it is converted to a load of 10 kN/m^2 appling on the corresponding beams. The live load on floors of 2 to 4 layers is 5 kN/m^2. The live load on the roof (without people) is 0.5 kN/m^2.

The soil is assumed as a homogeneous soil layer. Plate unit is used for primary support, tunnel face, and temporary steel. Entity unit is used for frame, foundation, pre-reinforcement area and soil body. Mohr - coulomb model is used as the constitutive model of pre-reinforcement area and soil body. The linear elastic model is adopted for primary support, tunnel face and temporary steel frame, frame and foundation. The material parameters adopted here are shown in Table 1.

Table 1 Material parameters of soil and structures

Constructional element	Gravity /kN·m^{-3}	Elasticity modulus /MPa	Poisson's ratio	cohesive force /kPa	Internal friction angle /°
Soil body	18.5	18	0.38	12	15
Pre-reinforcement area	21	100	0.30	30	35
Preliminary bracing (before setting)	25	10000	0.20		
Preliminary bracing (after aetting)	25	28000	0.20		
Tunnel face	25	10000	0.20		
Temporary steel	78	200000	0.17		
Frame	25	30000	0.20		
Foundation	25	31500	0.20		

The length of the entire model is 80 m and width of 40 m and height of 60 m. The tunnel crosses the buildings transversely, and L is assumed as the distance between the tunnel axis and the buildings. Under the standard operating mode, L equals to 0 m. As shown in Fig.1, transverse framework is named as 1, 2, 3, 4, 5, 6 and longitudinal framework named A, B, C for the convenience of description. The excavation distance is assumed as y=0 m when the excavation face reach the foundation edge of the building. The y is assumed to be negative and positive respectively before and after the arrival of the excavation face. The meshed elements are shown in Fig.2.

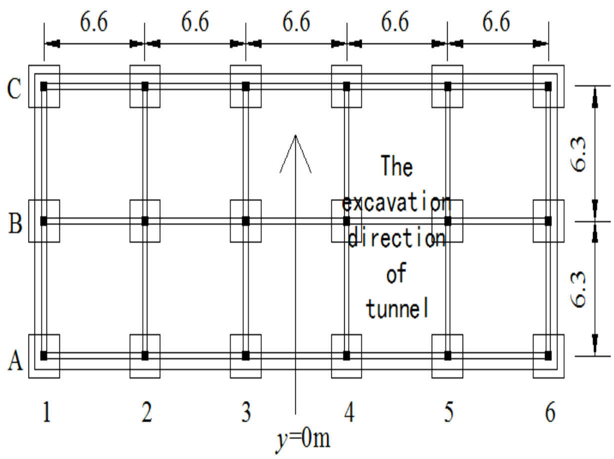

Fig. 1. Sketch of foundation location (unit: m)

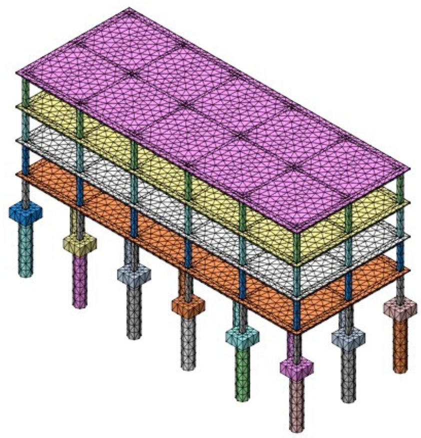

(a) Building model

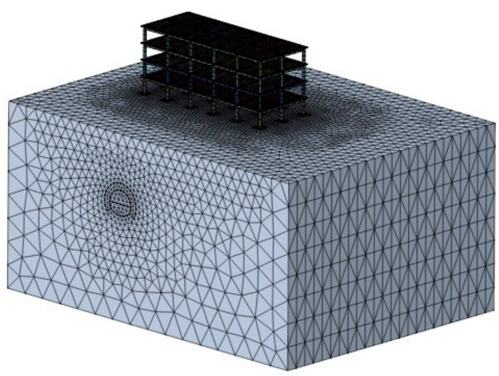

(b) The overall model

Fig. 2. Meshing diagram

2.2 Construction process simulation of shallow-buried underground excavation tunnel

The present paper assumes that: (1) the osmosis of groundwater is ignored and soil deformation will not change with time; (2) the coordinate method is adopted for the structure-foundation and foundation-soil deformation calculation; (3) the surface settlement before tunnel excavation is zero, i.e., the surface settlement caused by the building gravity is neglected.

The Simulation are followed as: (1) to activate the soil, and initiate the self-weight load and reset displacement; (2) to modify the properties of basic elements and activate the structure elements; then apply the building load and reset displacement; (3) to modify the pre-reinforcement element properties and accomplish the simulation process of the pre-reinforcement; (4) to carry out the soil excavation in the upstairs and activate intermediate steel element, upper tunnel face element, and the upper primary support element; (5) to modify the properties of the upper primary support element and simulate the primary support stiffness; (6) to initiate the soil excavation to the ground and activate tunnel face element and primary lower support element; (7) to modify the lower element attributes of the primary support.

3. Analysis by the finite element method

3.1 Displacement analysis (L=0 m)

Figure 3 shows the subsidence of the outer edge of the first floor which is the first crossed part by the tunnel. As shown in the figure, the building has little subsidence before the tunnel excavation face passes across the building. The soil settlement is relatively uniform and the difference of settlements between side- and middle ground is not significant. When the excavation surface arrives the building, the building subsidence becomes increase. The settlement is most obvious from y=-6 m to y=12 m, and the effect of construction should be noted. When y=20.6 m, the excavation surface in the lower steps penetrates through the foundation of the structure, and the settlement turns to stable. When the excavating distance reaches y=36 m, the settlement of the structure becomes stable. It is indicated that influential area of the shallow-buried underground excavation tunnel is large. The foundation subsidence curve is normally distributed. The maximum subsidence amount is 22.9 mm and the maximum differential subsidence is 11.9 mm. This phenomenon suggests that the overall stiffness of the short-pile foundation is insignificant.

Figure 4 shows the subsidence of the foundations of A4, B4, C4 during the tunnel excavation near the axis of vertical cushion cap. In the figure, A4 refers to the intersection of cap in row A and that in row 4. It can be seen from the figure that, before the excavation surface of the tunnel reaches the edge of foundation, the difference of settlement in the three-span frame is insignificant. After that, the variation of settlement in frame A4 increases, the settlement of B4 and C4 increases in sequence y and the difference of settlement in the three-span frame increases. When y=10 m, the difference of settlement in frame A4 and B4 reaches the maximum value of 4.9 mm and for frames B4 and C4, 4.7 mm. The difference of settlement in the three frames reduces afterward, and approaches 0 when y=36 m. This finding suggests that short-term uneven settlement in the structure occurs in the direction of tunnel excavation. The range of influence is relatively large (about 40 m) and the difference of settlement is largest when excavation is conducted underneath the structure.

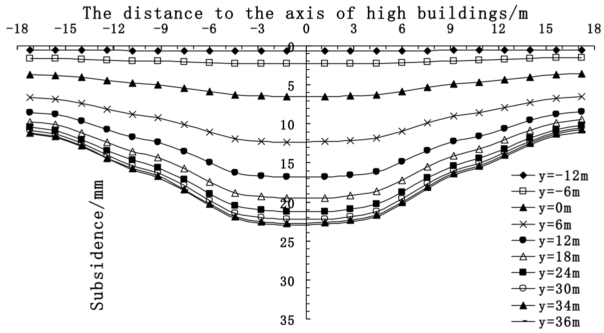

Fig. 3. Settlement of the outer edge of wall at ground floor in the tunnel excavation process

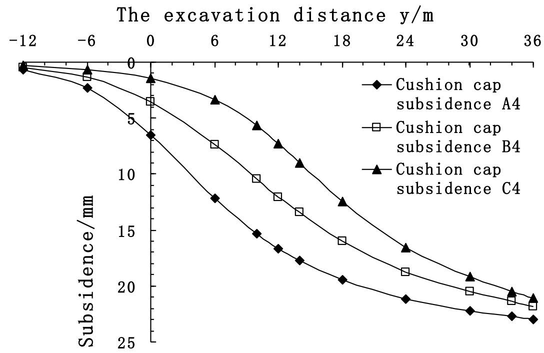

Fig. 4. Settlement of vertical cushion cap in the tunnel excavation process

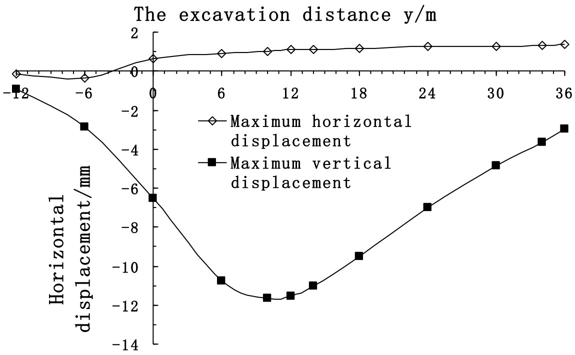

Fig. 5. Maximum value of horizontal frame displacement in the process of tunnel excavation

Figure 5 shows the relationship between the maximum horizontal displacement and the excavation distance, where the positive direction of the transverse horizontal displacement is the tunnel excavation direction, and the positive direction of the lateral horizontal displacement is the direction from left to right. Maximum horizontal displacement mainly appears at the top of the frame. As shown in the figure, the absolute value of the maximum transverse horizontal displacement is relatively small and will increase gradually with the increasing of the distance of excavation. The value became stable after y=18 m with an average of 1.3 mm. Maximum longitudinal horizontal displacement firstly increases then decreases. When y=10 m, maximum longitudinal horizontal displacement reaches the maximum value of 11.67 mm, the tilt rate of the building main body is 0.81 ‰ and less than 4 ‰, and thus, it fulfills the requirements of specification [17].

Figure 6 is the sketch (the figure center is the direction of tunnel excavation) of the vertical deformation of the buildings after amplification when y=10 m. The building will suffer horizontal and transverse deformations at this moment.

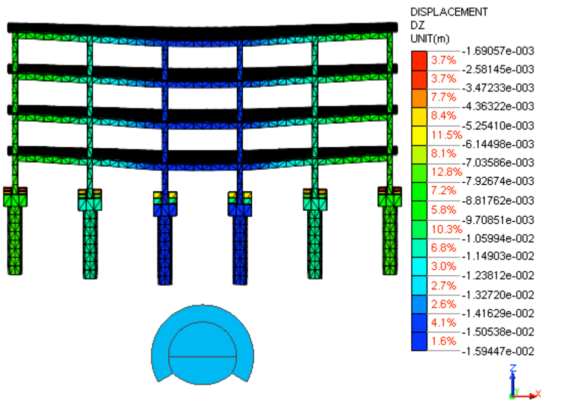

Fig. 6. Vertical deformation of the buildings after amplification (y=10 m)

3.2 Stress and strain (L=0 m)

The first principal stress of the component reflects of the phenomenon of tensile stress concentration. Based on code for design of concrete structures [18], the standard values of axial tension strength for C30 concrete is f_{tk}=2.01 MPa.

Figure 7 shows the curve of the first principal stress P_1 and the maximum deformation rate E_1 in the tunnel excavation process. As shown in the figure, the trends of both P_1 and E_1 are generally the same. When y<6m, P_1 and E_1 increase rapidly; when 6 m⩽y<14 m, the increase of P_1 and E_1 become gradual; when 14 m⩽y<34 m, the increase rate of P_1 and E_1 raise again; after y=34 m, P_1 and E_1 become stable. The maximum value of P_1 is 15.19 MPa, which is 7.6 times of f_{tk}. It is concluded that during shallow-buried and mining tunneling, the tensile stress in the structure would surpass the nominal axial tensile strength of the component, which would result in cracks [19]. Relevant procedures should be conducted during construction.

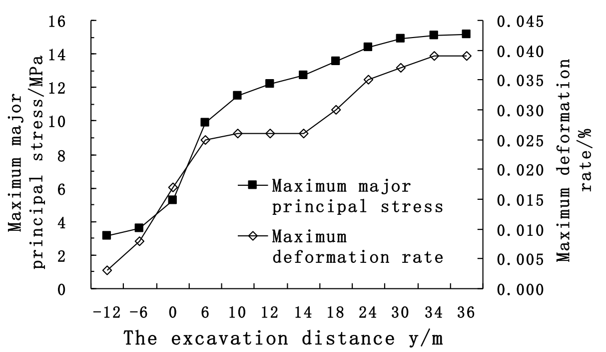

Fig. 7. Curves of P_1 and E_1 during the process of tunnel excavation

3.3 Soil conditions change

Numerical calculations are carried out considering three different types of soil conditions. The soil parameters are shown in Table 2, with L=0 m and y=36 m.

Table 2 Physical and mechanical parameters of soil

Name	Gravity /kN·m^{-3}	Elasticity modulus /MPa	Poisson's ratio	Cohesion /kPa	Internal friction angle /°
Floury soil	19.0	30	0.30	15	31
Clay	18.5	18	0.38	12	15
Soft clay	18.0	15	0.42	10	12

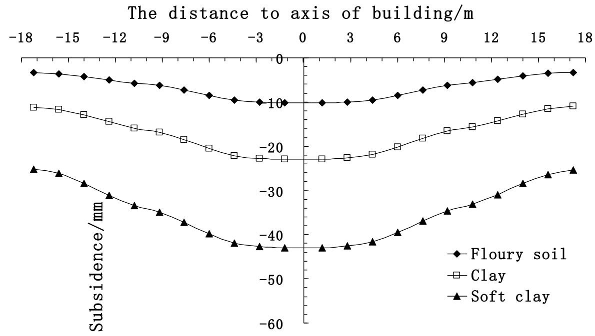

Fig. 8. Settlement curves of the outer edge of wall at ground floor under different soil conditions

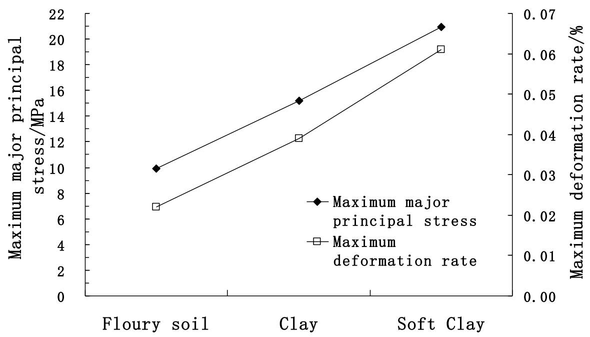

Fig. 9. Relationship of P_1 or E_1 and soil condition

Figure 8 shows the settlement curves of the outer edge of wall at ground floor where the tunnel first penetrated in different soil conditions. Figure 9 is the relationship curves of P_1 or E_1 under different soil conditions. It can be seen that, the settlement of structure increases with the deterioration of soil conditions. The maximum settlement of the three types of soil are 10.1 mm, 22.9 mm and 43.0 mm respectively; the difference of settlement between the edges and the middle of the wall at ground floor increases with the value being 6.7 mm, 11.7 mm and 17.9 mm, respectively. The P_1 and E_1 of the frame increase significantly, where P_1 increases by 110% and E_1 by 177%. This finding shows that cracking in the structure is more likely to occur under the poor soil condition.

Based on Code for design of building foundation [17], the allowable value difference of subsidence of frame structure is $0.002L_0$, where L_0 stands for the distance between the two column base centers. In the present paper, L_0 is 6.6 m. The permissible difference of subsidence is 13.2 mm. When the soil is soft clay, the maximum settlement difference in adjacent pile foundations is 9.23mm<13.2mm; when the soil is clay, the value is 6.94mm<13.2mm, which satisfies the requirement. According to the Chinese National Code for Designing Concrete Structures [18], the nominal axial tensile strength of C30 concrete is f_{tk} =2.01 MPa. The P_1 value of soft clay is 20.94 MPa which is about 10 times of f_{tk}. Therefore, cracking is likely to occur and damage the structure.

3.4 Change of the height of floors

Take L=0 m and y=36 m. The layer H=3, H=4 and H=5 are selected here to study the effect of the floor heights. Figure 10 shows the settlement curves of the outer edge of wall at ground floor for structures with different level height. Figure 11 shows the relationship curve between P_1 or E_1 and L under different layer height.

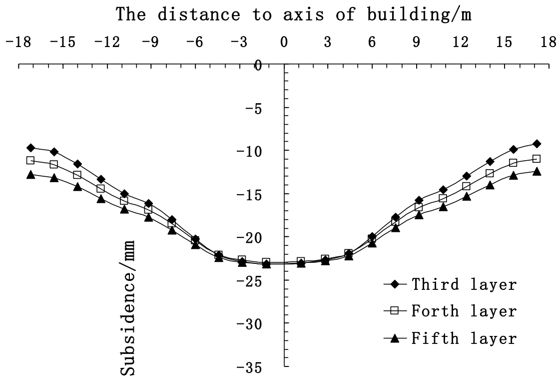

Fig. 10. Settlement curves of the outer edge of wall at ground floor under different height of floors

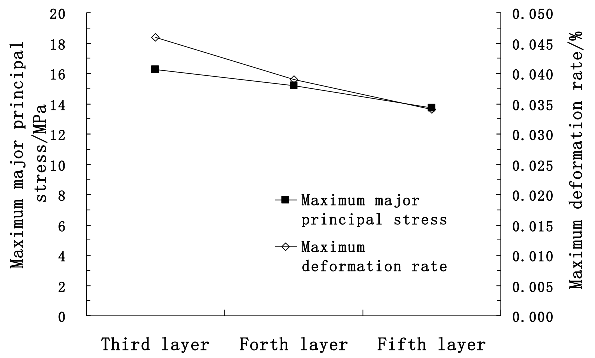

Fig. 11. Relationship between P_1 or E_1 and the height

As is shown in the figure, with the increase of height, the maximum settlement is almost the same with the value of 23.1 mm, 22.9 mm and 23.1 mm, respectively. The magnitude of increase is larger in the edges than in the middle. That is, the difference of settlement between the edges and the middle of wall at ground floor reduces with the value of 13.5 mm, 11.7 mm and 10.4 mm, respectively; Both P_1 and E_1 exhibit a reducing trend, where P_1 reduces by 16% and E_1 reduces by 26%, suggesting that with the increase of level height, the overall rigidity of the frame structure increases.

3.5 Horizontal position changes of tunnel and building

Figure 12 shows the settlement at the outer edge of the wall at ground floor with different value of L when y=36 m. As seen from Fig.12, when L=0 m, the foundation settlement curve appears to be axial symmetrical with a maximum settlement being 23 mm, and the entire structure is settled. With the increase of L, the structure inclines towards the tunnel, and the maximum foundation settlement increases and the location shifts towards the direction of movement of L; when L=17.5 m, the largest foundation settlement is happened with a value of 34 mm (the axis of the tunnel is located straight underneath the outer edge of the cap at this stage), and the structure is likely to be cracked or inclines. When L=32 m, the maximum foundation settlement is 5 mm. The overall difference of settlement in the structure is small which suggests that tunneling has little effect on the structure at this stage.

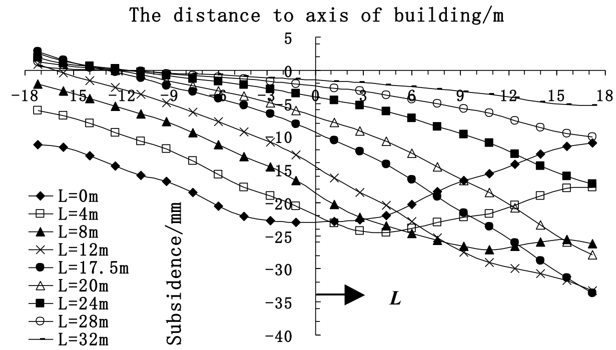

Fig. 12. Settlement of the outer edge of wall at ground floor in the process of tunnel excavation at different values of L

Figure 13 shows the relationship between P_1 or E_1 and L with y=34 m and changing L values. As shown in the figure, with the increase of L, the values of P_1 and E_1 generally reduce. When L=0 m, P_1 and E_1 reach the maximum value simultaneously, with the maximum value of P_1 being 15.19 MPa and E_1, 0.039%; when 0 m<L⩽12 m, the values of P_1 and E_1 reduce sharply; when 12 m<L⩽32 m, E_1 decreases gradually. When 12 m<L⩽24 m, P_1 decreases gradually; when L>24 m, the value of P_1 slightly increases.

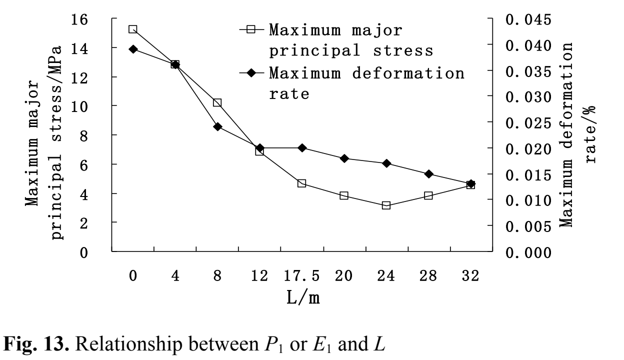

Fig. 13. Relationship between P_1 or E_1 and L

When L increases from 0, the absolute value of the maximum longitudinal horizontal displacement of the frame is relatively stable and reduces gradually with a maximum value of 3.7 mm. The value decreases towards 0 after y=24 m. The maximum transverse horizontal displacement increases at first and then decreases. When L=17.5 m, (the axis of the tunnel is located straight underneath the outer edge of the cap at this stage) a maximum value of 19.1 mm is witnessed. The global inclination of the structure at this time is 1.33 ‰ which is less than 4 ‰ [17].

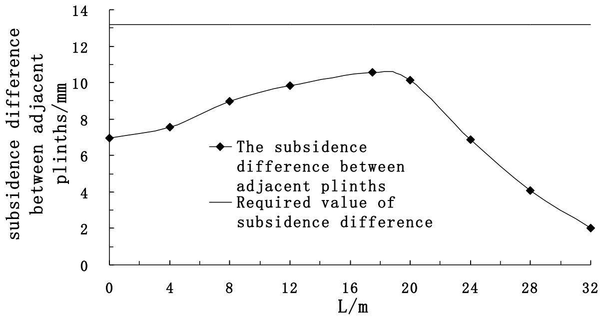

Fig. 14. Relationship of subsidence difference between adjacent plinths and L

As shown in Fig.14, the integrity of the short pile foundation is weak and therefore a large difference in settlement will occur. With the increase of L, the maximum subsidence difference between adjacent plinths shows a trend of firstly increasing and then decreasing, and reaches the maximum value of 10.6 mm when L=17.5 m. In the allowed value range in the specification [17], it means the buildings are safe.

4. Conclusions

When L=0m, with the excavation of shallow-buried and mining tunneling, the maximum settlement of the structure increases and the affected area in the longitudinal direction of the structure is large (about 40m). Since the global stiffness of the frame structure with short pile foundation is small, the difference of settlement between the edges and the middle of the structure is relatively large. When the values of P_1 and E_1 increase, the first principal stress in the structure exceeds the nominal tensile strength which may result in cracking in the structure.

For the poor condition of soil, the building subsidence and non-uniform subsidence become severe, and, P_1 and E_1 increase significantly. It is indicated that the poorer the soil is, on the more dangerous the structure becomes. With the increasing of floor height, the stiffness of the structure increases and the effect of tunneling on the structure reduce.

With the increase of L, the building will incline towards the tunnel. The P_1 and E_1 generally decrease, and the subsidence difference between adjacent plinths firstly increases and then decreases.

References

1. Gang Wei. “Prediction of soil settlement caused by double-line parallel shield tunnel construction”, *Disaster Advances*, 6(6), 2013, pp.23–27.
2. Dingli Zhang, Pengfei Li, Yanjuan Hou, Qian Fang. “Influence due to urban tunnel excavation on ground buildings and its countermeasures”, *Chinese Journal of Geotechnical Engineering*, China, 32(2), 2010, pp.296–302.
3. Anita Cerić, Danijela Marčić, Krešo Ivandić. “A risk-assessment methodology in tunnelling”, *Tehnički vjesnik – Technical Gazette*, 18(4), 2011, pp.529–536.
4. Chungsik Y, Jae-Hoon K. “A web-based tunnelling-induced building/utility damage assessment system: TURISK”, *Tunnelling and Underground Space Technology*, 18(5), 2003, pp.497–511.
5. Richard J. Finno, Frank T, Edwin Rossow, J. Tanner Blackburn. “Evaluating damage potential in buildings affected by excavations”, *Journal of Geotechnical and Geoenvironmental Engineering*, 131(10), 2005, pp.1199–1210.
6. Maleki M, Sereshteh H, Mousivand M, Bayat M. “An equivalent beam model for the analysis of tunnel-building interaction”, *Tunnelling and Underground Space Technology*, 26(4), 2011, pp.524–533.
7. Gang Wei. “Numerical analysis of DOT shield 45° crossing the masonry structure buildings”, *Disaster Advances*, 6(8), 2013, pp.20–25.
8. Burd H J, Houlsby G T, Augarde C E, Liu G. “Modelling tunnelling-induced settlement of masonry buildings”, *Proceedings of the ICE-Geotechnical Engineering*, 143(1), 2000, pp.17–29.
9. Mroueh H, Shahrour I. “A full 3-D finite element analysis of tunnelling-adjacent structures interaction”, *Computers and Geotechnics*, 30(3), 2003, pp.245–253.
10. Jenck O, Dias D. “3D-finite difference analysis of the interaction between concrete building and shallow tunnelling”, *Geotechnique*, 54(8), 2004, pp.519–528.
11. Shaoming Liao, Jianhang Liu, Rulu Wang, Zhiming Li. “Shield tunnelling and environment protection in Shanghai soft ground”, *Tunnelling and Underground Space Technology*, 24(4), 2009, pp.454–465.
12. Pickhaver J A, Burd H J, Houlsby G T. “An equivalent beam method to model masonry buildings in 3D finite element analysis”, *Computers and Structures*, 88(19-20), 2010, pp.1049–1063.
13. Mirhabibi A, Soroush A. “Effects of surface buildings on twin tunnelling-induced ground settlements”, *Tunnelling and Underground Space Technology*, 29(5), 2012, pp.40–51.
14. Gang Wei, Xingu Qiu, Xinjiang Wei. “Numerical simulation of underground excavated tunnel construction of adjacent structure”, *Rock and Soil Mechanics*, 30(2), 2009, pp.547–552.
15. Zude Ding, Limin Peng, Chenghua Shi. “Analysis of influence of metro tunnel crossing angles on ground buildings”, *Rock and Soil Mechanics*, 32(11), 2011, pp.3387–3392.
16. Branimir Rončević, Goran Turkalj. “Application of plastic hinges in finite element analysis of framed structure”, *Engineering Review*, 26(1/2), 2006, pp.75–87.
17. China Academy of Building Research. GB50007-2011 Code for design of building foundation, Beijing, China, China Building Industry Press, 2011.
18. The Ministry of Construction of the People's Republic of China. GB50010-2010 code for design of concrete structures, Beijing, China, China Building Industry Press, 2010.
19. X.B. He, B Yan, J.Y. Gu, Q Shen. “Crack-arresting and strengthening mechanism of hybrid fiber reinforced polymer sheets in strengthening of reinforced concrete beams”, *Journal of Engineering Science and Technology Review*, 6(2), 2013, pp.134–138.